https://doi.org/10.5194/essd-2020-57
Preprint. Discussion started: 15 April 2020

Open Access Earth System Science Data Discussions

Annual 30-meter Dataset for Glacial Lakes in High Mountain Asia from 2008 to 2017

Fang Chen[1,2,3], Meimei Zhang[1], Huadong Guo[1,2,3], Simon Allen[4,5], Jeffrey S. Kargel[6], Umesh K. Haritashya[7], C. Scott Watson[8]

[1]Key Laboratory of Digital Earth Science, Aerospace Information Research Institute, Chinese Academy of Sciences, No. 9 Dengzhuang South Road, Beijing 100094, China.

[2]State Key Laboratory of Remote Sensing Science, Aerospace Information Research Institute, Chinese Academy of Sciences, No. 9 Dengzhuang South Road, Beijing 100094, China.

[3]Hainan Key Laboratory of Earth Observation, Aerospace Information Research Institute, Chinese Academy of Sciences, Sanya 572029, China.

[4]Department of Geography, University of Zurich, Zurich, 8057, Switzerland.

[5]Institute for Environmental Sciences, University of Geneva, Geneva 1205, Switzerland.

[6]The Planetary Science Institute, Tucson, Arizona, 85719, USA.

[7]Department of Geology, University of Dayton, Dayton, Ohio, 45469, USA.

[8] Department of Hydrology & Atmospheric Sciences, University of Arizona, Tucson, Arizona, 85721, USA.

Correspondence to: Meimei Zhang (zhangmm@radi.ac.cn)

Abstract. Climate change is intensifying glacier melting and lake development in High Mountain Asia (HMA), which could increase glacial lake outburst flood hazards and impact water resource and hydroelectric power management. However, quantification of variability in size and type of glacial lakes at high resolution has been incomplete in HMA. Here, we developed a HMA Glacial Lake Inventory (Hi-MAG) database to characterize the annual coverage of glacial lakes from 2008 to 2017 at 30 m resolution using Landsat satellite imagery. It is noted that a rapid increase in lake number and moderate area expansion was influenced by a large population of small glacial lake (≤0.04km^2), and faster growth in lake number occurred above 5300 m elevation. Proglacial lake dominated areas showed significant lake area expansion, while unconnected lake dominated areas exhibited stability or slight reduction. Small glacial lakes accounted for approximately 15% of the lake area in Eastern Hindu Kush, Western Himalaya, Northern/Western Tien Shan, and Gangdise Mountains, but contributed >50% of lake area expansion in these regions over a decade. Our results demonstrate proglacial lakes are a main contributor while small glacial lakes are an overlooked element to recent lake evolution in HMA. Regional geographic variability of debris cover, together with trends in warming and precipitation over the past few decades, largely explain the current distribution of supra- and proglacial lake area across HMA. The Hi-MAG database are available at: https://doi.org/10.5281/zenodo.3700282 (Chen et al., 2020), it can be used for studies on glacier-climate-lake interactions, glacio-hydrologic models, glacial lake outburst floods and potential downstream risks and water resources.

https://doi.org/10.5194/essd-2020-57
Preprint. Discussion started: 15 April 2020

Open Access Earth System Science Data Discussions

1 Introduction

High Mountain Asia (HMA) consisting of the whole Tibetan Plateau and adjacent mountain ranges such as Himalaya, Karakoram, and Pamirs, covers the largest area of mountainous glaciers globally. HMA has significant but variable overall glacier retreat and downwasting (Brun et al., 2017;Bolch et al., 2012), yet glacial lakes have been incompletely documented. Glacial lake development varies according to climatic, cryospheric, and lake-specific conditions, such as basin geometry that is either connected to glaciers or unconnected, and the length of the lake/glacier contact. Previous assessments of HMA glacial lake development focused mainly on large lakes (Haritashya et al., 2018;Salerno et al., 2012), covered few temporal intervals (Brun et al., 2017;Gardelle et al., 2011) or were narrowly scoped geographically (Haritashya et al., 2018;Aparna et al., 2018). However, a homogeneous, annually resolved inventory and analysis of the spatial and temporal extent of small lakes and different types of glacial lakes over the entire HMA has been lacking. We developed a HMA Glacial Lake Inventory (Hi-MAG) database to characterize the annual coverage of glacial lakes from 2008 to 2017 at 30 m resolution. 40,481 Landsat scenes were processed using Google Earth Engine (GEE) cloud computing to delineate glacial lakes (located within a 10 km from the nearest glacier terminus) larger than nine (e.g., 3 x 3) pixels (0.0081 km^2) (Nie et al., 2017).

Lakes were manually classified into four categories representing different formation mechanisms or growth stages (Fig. A1): i) proglacial lakes, usually connected to the glacial tongue and dammed by unconsolidated or ice-cemented moraines; ii) supraglacial lakes - this is where ponds form in depressions on low-sloping parts of the surface of a melting glacier and are dammed by ice or the end-moraine or stagnating glacier snout; iii) unconnected glacial lakes, which are glacial lakes not directly connected to their parent glaciers at the present time but which, to some extent, may be fed by at least one of the glaciers located in the basin and may have been (but not necessarily are) recently detached from ice contact due to glacial recession. Although not directly connected with the parent glaciers, these glacial lakes are also the outcome of glacier melting in response to climate warming, they can supply fresh water to major river systems of the HMA region, and their changes have significant scientific and socio-economic implications (Nie et al., 2017;Song et al., 2016); and (iv) ice-marginal lakes, bounded by a lateral moraine on one side and damming glacier ice on the other side, or in some cases may form where a glacier tributary detaches from a main trunk glacier. We note that such ice-marginal lakes are very common in some parts of the world (e.g., Alaska) but are not common in HMA.

Every lake was cross-checked manually for potential automatic mapping errors. We defined an uncertainty of 1 pixel for the detected glacial lake boundaries, and calculated the systematic errors for the whole HMA region. We also assessed the inventory for climatic and geomorphological influences on lake distribution across HMA.

2 Study area and data

The study area covered the whole of High Mountain Asia, including the Himalayas, the Hindu Kush, Karakoram, Pamir Alay, Kunlun Shan and Tien Shan, etc (Fig. 4a). For this study, glacial lakes are formed and developed temporally with the retreat or thinning of glaciers and are directly or indirectly fed by glacier meltwater, they are located within a 10 km from the nearest glacier terminus (Zhang et al., 2015;Wang et al., 2013). Approximately 40,481 Landsat series satellites scenes including Landsat 5 TM imagery during 2008 to 2011, Landsat 7 ETM+ imagery in 2012, and Landsat 8 OLI during 2013 to 2017, were available in GEE and were used to produce the annual glacial lake maps over the entire HMA (Fig. 1). Here, when Landsat 5 or 8 data were available, Landsat 7 ETM+ imagery with SLC-off gaps were generally excluded due to their artefacts induced by the slatted appearance of the original images, but were exclusively used for the glacial lake mapping in 2012 since no other

https://doi.org/10.5194/essd-2020-57
Preprint. Discussion started: 15 April 2020

Open Access Earth System Science Data Discussions

Landsat data were acquired that year. For the years before 2008, the year-round Landsat 5 TM data in many years (e.g., 2004, 2005, 2006, and 2007) do not fully cover the HMA region.

The SLC-off condition of Landsat ETM+ also introduces artefacts because the slatted appearance of the original images is occasionally carried into the glacial lake map in 2012. Lakes out of the gaps were accurately classified but usually misclassified otherwise. Techniques to fill the SLC-off gaps exist, but these create artificial values that will result in the false water detections (Chen et al., 2011). Considering the strong spatial and temporal variability of glacial lakes like supraglacial lakes, techniques which merge data from one or more SLC-off fill scenes for generation of a gap-free image require careful use, even using the thousands of Landsat ETM+ images. It is noted water mapping using multi-temporal time series images at large scales usually avoided the use of such techniques (Mueller et al., 2016). In this study, errors caused by striped gaps of Landsat ETM+ were manually corrected using additional high-quality scenes during the whole year with assistance of images from adjacent years.

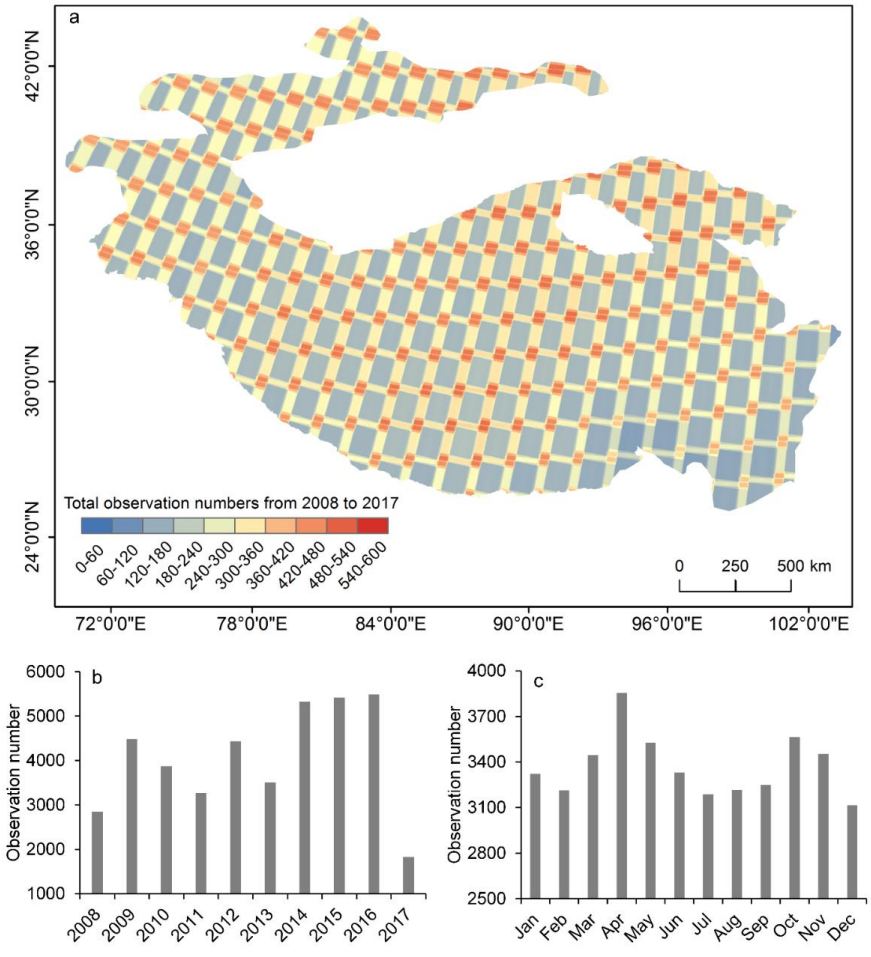

Fig. 1. (a) The distribution of total observation numbers from all GEE Landsat scenes by (b) year and (c) month.

https://doi.org/10.5194/essd-2020-57
Preprint. Discussion started: 15 April 2020

3 Methods

3.1 Satellite imagery selection strategy

To reduce the influence of seasonal lake fluctuations for the mapping, one effective solution is to map glacial lakes and measure their long-term changes during stable seasons when lake extents are minimally affected by meteorological conditions and glacier runoff. Here the selected time series of Landsat data were generally from July to November. During this period of each year, the Landsat imagery featured less perennial snow coverage. The lakes also reached their maximum extent, specifically around the end of the glacier ablation season (June to August) (Gardelle et al., 2013;Liu et al., 2014)- except in the central and eastern Himalaya, where peak ablation extends into most-monsoon September and October. In monsoon-affected areas such as Nepal and Bhutan, monsoon cloud cover in July to mid-September means that most of those areas are covered by clear-sky images only from late September to November. Southeast Tibet regions are problematic not only because the observation season is short but abundant cloud cover, which is formed by the warm humid airflow raised by topography (Haritashya et al., 2018;Qiao et al., 2016).

To further increase data availability, we set two criterions for the selection of imagery with valid observations over the potential glacial lake area by using the cloud score functions in GEE, including (i) a partial Landsat scene that has less than 20% clouds in the 10 km buffer around each glacier outlines, or (ii) less than 20% cloud cover for the entire scene. If none of these criterions will get valid observations, then optimal mapping time needs to be broaden.

Although the selected image seasons are slightly different due to the meteorological conditions in different regions, they all comply with the same criterion that lake area were in clear-sky images and has small snow coverage, which will ensure the initial reliability of the mapping glacial lakes through GEE cloud computing platform.

3.2 Adaptive glacial lake mapping method

For the development of HMA Glacial Lake Inventory (Hi-MAG) database, we applied a systematic glacial lake detection method that combined two steps from initial glacial lake extraction and subsequently manual refinement of lake mapping results. The initial lake extraction was performed using Google Earth Engine cloud computing platform (https://earthengine.google.org/), which synchronizes all the Landsat data and also provides a consolidated environment for parallel computing and for the processing of the huge amounts of data covering large study areas.

The main procedures for glacial lake mapping using Landsat data are (Fig. 2): (i) the Landsat top of atmosphere data were clipped according to the extent of the glacier buffers and assembled into a time-series dataset; (ii) poor quality observations were identified - these included areas affected by cloud, cloud shadow, topographic shadow, SLC-off gaps. Fmask has the advantage of being able to process a large number of images in a more computationally efficient way. Here we used the Fmask routine (Zhu and Woodcock, 2012) to detect the clouds and cloud shadows in an imagery. Topographic shadows were then masked using the slopes (larger than 10°) and shaded relief maps (value less than 0.25) calculated from SRTM data (Li and Sheng, 2012;Quincey et al., 2017). This will remove considerable mountain shadows that have the similar spectral reflectance with water bodies. However, the derived slopes and shaded relief cannot fully represent the conditions on the date a given Landsat scene is acquired, some mountain shadows that interfere with the mapping results of glacial lakes from GEE still remains; (iii) the modified Normalized Difference Water Index (MNDWI) were calculated (Hanqiu, 2006); (iv) the potential glacial lake areas were extracted by applying adaptive MNDWI threshold (Li and Sheng, 2012). Because of the spatial resolution of Landsat data and the relative stability of glacial lakes, only lakes larger than nine pixels (≥ 0.0081 km^2) were

https://doi.org/10.5194/essd-2020-57
Preprint. Discussion started: 15 April 2020

considered in this study; and (v) manual inspection and refinement of individual glacial lake were conducted and the related attribution (i.e., lake type, elevation, distance to the nearest glacier terminus, area and perimeter) were added for each lake.

To ensure the quality of inventory, strict quality control was conducted to visually inspect and correct the mapping errors after the automated processing using GEE. False lake features, mainly identified as mountain shadows and river segments, were manually removed by overlapping mapped lake shorelines on the source Landsat imagery and higher-resolution imagery in Google Earth. For missing glacial lakes, the lake boundaries were edited further using ArcGIS. Furthermore, a cross-check and modification was conducted for each glacial lake based on the lake mapping results in conjunction with multi-temporal Landsat imagery. Here all the Landsat imagery that used for the inspection were downloaded manually from USGS Earth Explorer website (https://earthexplorer.usgs.gov/). Outputs per lake vector includes the information about lake type, elevation, distance to the nearest glacier terminus, area and perimeter. Meanwhile, each mountain range was characterized individually by utilizing the mountain boundary shapefile in High Mountain Asia (geo.uzh.ch/~tbolch/data/regions_hma_v03.zip).

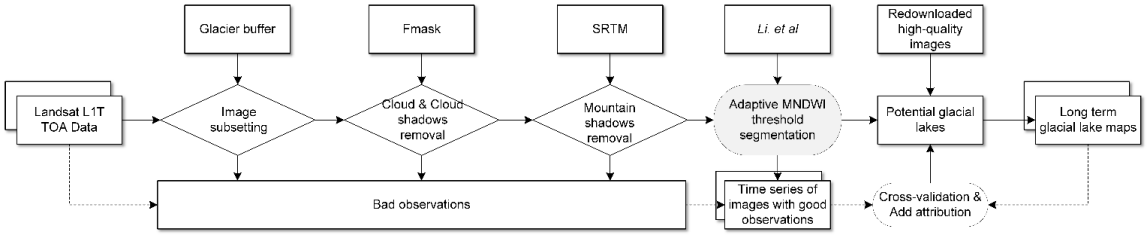

Fig. 2. Diagram of the glacial lake mapping workflow.

3.3 Yearly lake area changes calculations

Based on the final generated lake inventory data, we used the slope of linear regression of lake area (over the grid cell of 1°×1°) versus image date to qualify the yearly lake area changes during the study period. The approach to change analysis was predicted on using a Theil-Sen estimator, which chooses median slope among all the derived fitted lines to smooth the annual time series of data (Kumar, 1968;Song et al., 2018) Although the lake mapping was mainly conducted in the same period to ensure year-to-year consistency to the degree possible, the smoothing approach was still necessary because of the annual variation in the lake extent attributable to a variety of sources including adverse weather conditions, varying lake characteristics and image quality (Bhardwaj et al., 2015;Thompson et al., 2012). As such, conventional linear trends for the annual layers to estimate year-to-year changes is not reliable. For the glacial lake area time series in each 1°×1°grid, we applied the Theil-Sen estimator to derive the slope (annual change) of the trend. The upper and lower change estimates that satisfy the 90% confidence interval for the slope were also derived (Fig. A2). It should be noticed that the derived Theil-Sen trend can effectively represent long-term area changes due to its robustness for the trend detection and insensitivity to outliers, which is useful for the elimination the effect of differences in the sensor capabilities.

4 Cross-validation and uncertainty estimate

Accuracy assessment of the mapping results is difficult due to the lack of field measurements of glacial lakes in the continental-scale area like HMA. To obtain the quality controlled data, the glacial lake vector over the entire HMA for the years from 2008 to 2017 has been rechecked and reedited individually through dynamic cross-validation by ten trained

https://doi.org/10.5194/essd-2020-57
Preprint. Discussion started: 15 April 2020

experts, which is a time consuming process but are essential to maximize the quality of glacial lake change detection. On these conditions, an additional random validation samples were not selected and thus not used for the calculation of accuracy metrics like other mapping results using image extraction algorithm (Huan et al., 2016;Feyisa et al., 2014;Zhang et al., 2017).

For the estimation of the uncertainty of glacial lake area, a key influence factor is the spatial resolution of satellite data. In this study, the uncertainty of the glacial lake area was estimated as an error of ±1 pixels on either side of the delineated lake boundary. The percentage error of area determinations, A_{er}, then is proportional to sensor resolution and is given by (Krumwiede et al., 2014):

$$A_{er} = 100 \cdot (n^{1/2} \cdot m) / A_{gl} \quad (1)$$

Where n refers to the number of pixels defining the perimeter, approximated by the ratio of the perimeter length and sensor resolution, m is the areal spatial resolution of the sensor (m^2), A_{gl} is the lake area (m^2) and the factor 100 is there to convert to percentage.

Assuming an uncertainty of 1 pixel for the detected glacial lake boundaries, we calculated the systematic errors for the whole HMA region (Table 1). For the year between 2008 and 2017, the area uncertainty generally ranged from 0.1% to 50%, with the mean value falling around the 18%, and standard deviation around 11%. Most of the large glacial lakes (area ≥ 0.04km^2) have the mean area uncertainty of about 7%. This systematic error was more significant for the small-sized glacial lakes. We measured glacial lake down to 0.0081 km^2 (nine pixels in Landsat imagery), where systematic errors calculated by equation (1) were ~50%. Besides, it should be noted that in this study the smallest glacial lake detectable in the Landsat satellite data was set to nine connected pixels. Although a much smaller minimum mapping unit will create a greater number of glacial lakes over the study area, it will also bring proportionally larger uncertainty than large lakes at the same resolution.

Though the statistical systematic errors as computed are very large for the small lakes, it must be noted that the precision, as formulated by Krumwiede et al. (Krumwiede et al., 2014) and implemented in Haritashya et al. (Haritashya et al., 2018)is a much smaller error bar. Precision is reduced from the systematic error by a factor of square root of the number of perimeter pixels defining a lake. Also because the type of data (Landsat images) used in this study is similar, the precision of measurement (such as ability to detect area changes) is predictably much better than the accuracy.

Table 1. Area uncertainty (%) of glacial lakes for each year from 2008 to 2017.

Year	Min (%)	Max (%)	Mean (%)	Standard deviation (%)
2008	0.12	52.01	16.90	11.34
2009	0.12	58.41	18.81	11.77
2010	0.12	49.31	16.58	10.67
2011	0.12	58.32	18.04	11.55
2012	0.10	50.62	18.17	11.57
2013	0.10	50.62	18.14	11.38
2014	0.10	50.62	18.10	11.50
2015	0.10	50.62	17.96	11.10
2016	0.10	67.21	18.87	11.62
2017	0.10	50.98	18.74	11.46

https://doi.org/10.5194/essd-2020-57
Preprint. Discussion started: 15 April 2020

Open Access Earth System Science Data Discussions

5 Results

5.1 Distribution of various types and sizes of glacial lakes

The area coverage of glacial lakes increased by 98.22 km^2 between 2008-2017, a +6.39% change relative to 2008 (1537.71 km^2) (Fig. 3a). A linear least-squares fit to all the data showed a mean expansion rate of 18 km^2 a^{-1} for the 10-year record (Fig. 3a). Meanwhile, the estimated changes in glacial lake number from 2008 (11,524 lakes) to 2017 (14,477 lakes) showed an average increase of 380 lakes a^{-1}. The steeper percentage increase in lake number (30.73%) compared to a slower area expansion (11.07%) based on their linear fit trends showed that many small glacial lakes formed over this decade (Fig. A3). The number of lakes increased most rapidly above 4300 m a.s.l., especially above 5300 m (Fig. 3b). The increase of proglacial lakes was concentrated above 4900 m (Fig. 3c). Unconnected glacial lakes grew very slightly in total area below 4400 m (Fig. 3d), but increased at higher elevations. Glaciers are retreating and thinning at ever-higher elevations (Nie et al., 2017), causing the formation of new supraglacial lakes at high-elevation, expansion of existing ice-contact lakes, and detachment of glaciers from some lakes.

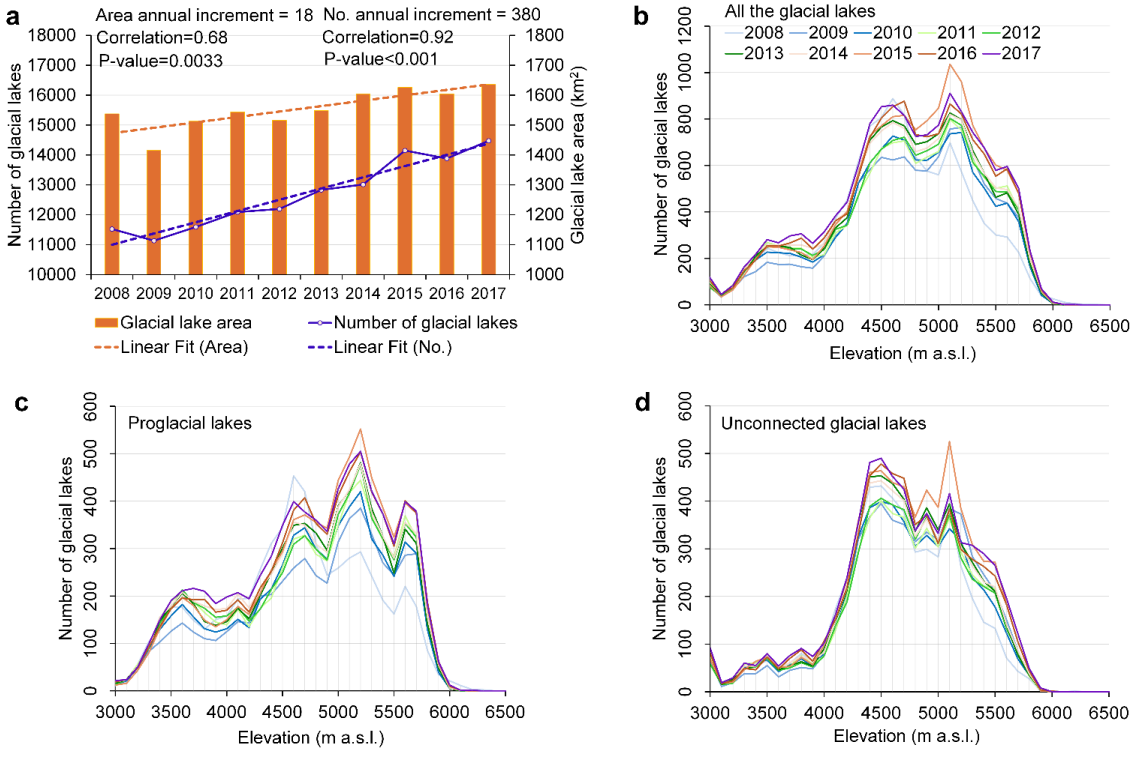

Fig. 3. Annual glacial lake number and area. (a) Total number and area of glacial lakes for HMA between 2008-2017. The annual increment is the slope of the trend of annual lake area and number. Altitudinal distribution (100-m bin sizes) of lake numbers for **(b)** all glacial lakes, **(c)** proglacial lakes, and **(d)** unconnected glacial lakes.

Annual changes in glacial lakes were further analyzed spatially using a 1°×1° grid over 22 mountain regions using non-parametric trend analysis (Fig. 4a). An analysis on mountain-wide lake area loss/gain from 2008 to 2017 for various lake types and sizes was conducted (Table A1, A2, and A3). Negative or undiscernible changes in glacial lake area were observed

https://doi.org/10.5194/essd-2020-57
Preprint. Discussion started: 15 April 2020

in the Eastern Tien Shan, Western Pamir, Tibetan Interior Mountains, and Eastern Tibetan Mountains (Fig. 4b), thus reducing overall increasing glacial lake area in HMA. The Eastern Tibetan Mountains lost 5.36 km^2 of lake area (Table A1), with the most negative area change (-0.55 km^2 a^{-1}) near 34°N, 101°E. Glacial lakes in Tanggula Shan and Eastern Himalaya exhibited large patches of area loss and gain. In contrast, Eastern Hindu Kush, Western Kunlun Shan, Western and Central Himalaya, and Nyainqentanglha showed rapid lake area increases. Between 2008 and 2017 Central Himalaya's glacial lake area increased by 38.86 km^2 (Table A1), exhibiting both a high density of 46 glacial lakes per 100 km^2 in 2017 and rapid growth, +1.18 km^2 a^{-1}, in lake area due to retreat and thinning of debris-covered glaciers (Fig. A4) (Song et al., 2016). Moderate area gains occurred along most of the Pamir Alay and Tien Shan, e.g., +0.49 km^2 a^{-1} in Central Tien Shan. The Hengduan Shan lakes had an area growth rate of +0.018 km^2 a^{-1}. Glacial lake area in Qilian Shan was spatially and temporally invariant across the whole observation record.

We found that glacial lakes exhibited different expansion trends for different lake types and supraglacial and ice-marginal lakes have relative few coverage areas comparing with proglacial and unconnected lakes (Fig. 4c). In the Eastern Hindu Kush and Central Himalaya, around half of the glacial lake area consisted of proglacial lakes, where most growth occurs (Fig. 4b). In the negative lake growth (shrinkage) regions of Tibetan Interior Mountains and Tanggula Shan, the unconnected glacial lakes were dominantly occupied. Proglacial lakes contributed approximately 83% of total area increase (81.47 km^2) over HMA (Table A2 and A3). Proglacial lakes in the Central Himalaya, Eastern Himalaya, and Western Himalaya, accounted for >54% of the total area increase (53.91 km^2). In general, proglacial lakes are a main contributor to recent lake evolution in HMA.

We noted the largest area growth of lakes occurred in areas with relatively large proportion of small glacial lakes, mainly due to rapid growth of existing lakes and new lake formation, whereas many large-lake dominated areas exhibited decreased or nearly unchanged lake extent (Fig. 4d). For example, small glacial lakes ($\leq$ 0.04 km^2) accounted for only 2% of lakes' area in the Tibetan Interior Mountains (Table A4), where glacial lakes in parts of the region shrank in area (Fig. 4b). 26% of small glacial lakes exhibited in the Eastern Hindu Kush, giving that region a high area growth rate.

It is noted opposite regional lake evolution results may be obtained comparing with the previous studies, which the contributions of small lakes were overlooked due to incomplete records of these small lakes for the HMA. For example, small glacial lakes showed significant contributions of >50% of the total area increase in Eastern Hindu Kush, Western Himalaya, Northern/Western Tien Shan, and Gangdise Mountains (Table A2 and A3). 69.82% of lake area gain in Gangdise Mountains are from small proglacial lakes (3.98 km^2), but the region would showed area decrease for proglacial lakes when only taking into account medium or large proglacial lakes (-1.63 km^2). In Eastern Hindu Kush, medium/large proglacial and unconnected lakes exhibited decreased area (-0.47 km^2), however, the region showed increased lake area (2.86 km^2) when considering contributions of small proglacial and unconnected lakes (3.41 km^2).

https://doi.org/10.5194/essd-2020-57
Preprint. Discussion started: 15 April 2020

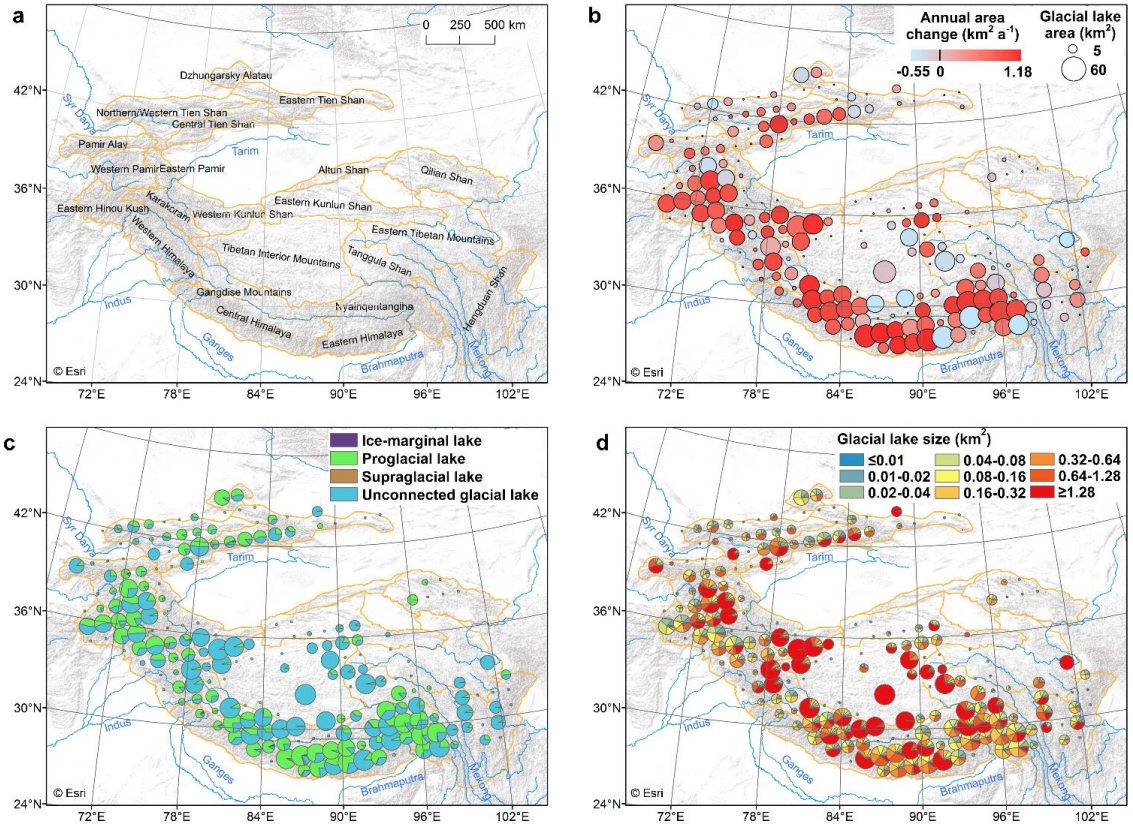

Fig. 4. Glacial lake area changes and area distribution. (a) Geographic coverage of mountain ranges in HMA. **(b)** Annual rate of change in lake area (2008-2017) on a 1°×1° grid. The size of the circle for the area in 2017. **(c)** Proportional areas of four types of glacial lakes in 2017. **(d)** Area of different sizes of glacial lakes in 2017. The terrain basemap is sourced from Esri (© Esri).

5.2 Inter-annual variability of small glacial lakes for different mountain regions

We further examined the inter-annual variations in the number of small glacial lakes for different HMA mountain regions (Fig. 5), which increased for many regions, such as North/Western Tien Shan, Eastern Hindu Kush, Central Himalaya, Eastern Himalaya, and Nyainqentanglha. The small glacial lakes in the Karakoram and Pamir Alay exhibited fluctuation (years of decrease but an overall increase) across the 10-year period, probably indicating meltwater lake drainage and refilling related to glacial and seasonal dynamics (Bhambri et al., 2013;Gardelle et al., 2013). Small lakes in the Hengduan Shan showed a rather constant number for all three sizes. For the Western Kunlun Shan, although the number of lakes slightly increased, the total number was small (about 20 or fewer glacial lakes for each size class). It is noted that the number of smallest lakes ($\leq$0.01km^2) grew very slightly in most of HMA regions and faster growth in lake number contributed by lakes that are between 0.01 km^2 and 0.04 km^2. Overall, small glacial lakes exhibited increasing trends in number in the regions with relative rapid area increases (Fig. 4b), and drove the pattern of lake number growth over the whole HMA region in the last decade.

https://doi.org/10.5194/essd-2020-57
Preprint. Discussion started: 15 April 2020

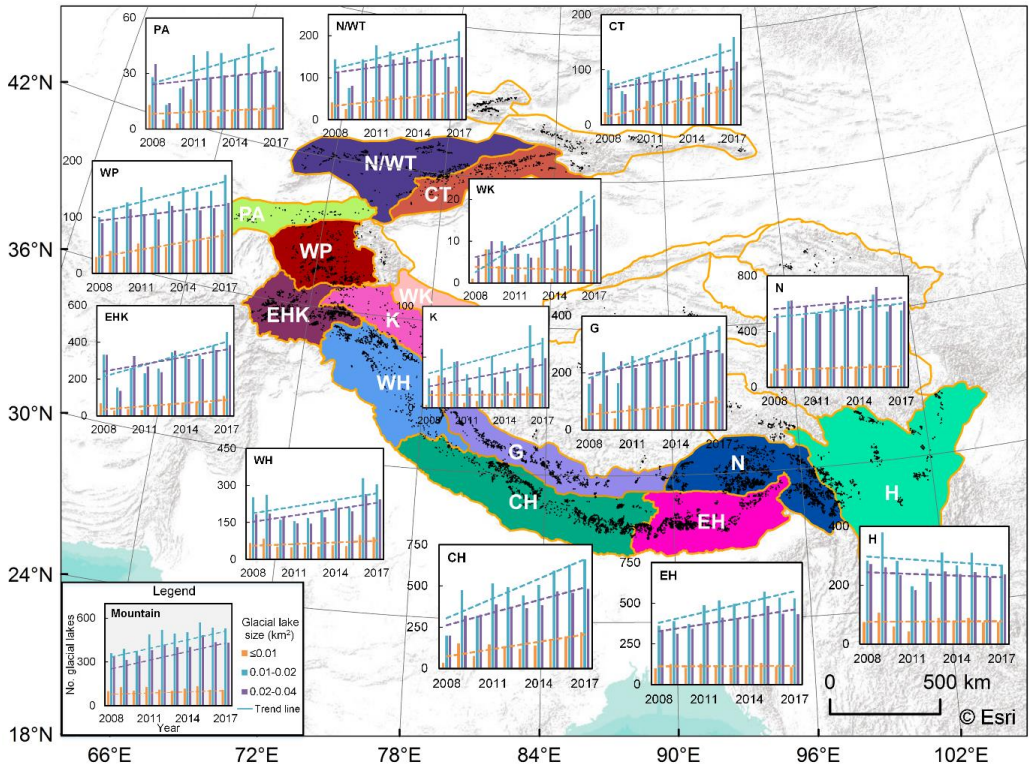

Fig. 5. Annually resolved changes in the number of small glacial lakes. The plotted area classes are (area ≤0.01km^2 (orange), 0.01 km^2＜area≤0.02 km^2 (blue), 0.02 km^2＜area≤0.04 km^2 (purple)). Note that the smallest size category has a narrow range of sizes starting at 0.0081 km^2 (nine 30 x 30 m pixels) and might also exhibit some incomplete detection due to image resolution limits. Glacial lake locations in 2017 are in black. The terrain basemap is sourced from Esri (© Esri).

5.3 Influencing factors of current distribution of glacial lakes

To explore potential factors that have influenced glacial lake distribution across HMA, we focus on proglacial and supraglacial lakes, for which the changes are closely related with glaciers and expansion is most rapid. Proglacial lakes frequently develop from the enlargement and coalescence of one or more supraglacial lakes (Haritashya et al., 2018;Thakuri et al., 2016). Proglacial and supraglacial lake development from 2008 to 2017 is strongly correlated to initial lake area in 2008 (R^2=0.53, Table A5); larger ice-contact proglacial lakes imply larger calving-front interactions.

For the years before 2008, the year-round Landsat 5 TM data in many years do not fully cover the HMA region. In this study we conducted inventory over a ten-year time period, which is shorter than typical glacier response times, lake expansion is not expected to couple with short-term climate trends (Bolch et al., 2012;Haritashya et al., 2018). In the inclusion of mass balance forcing of glacial lake changes, the same questions about the response times also occur. Hence, rather than focus on the short term evolution of lake expansion, we investigated if climate and other factors have influenced the overall distribution of lake area, as observed in 2017. To investigate factors influencing the predominance of proglacial and supraglacial lakes in the Nyainqentanglha, Eastern, and Central Himalayan regions in 2017, geomorphic, topographic and climate parameters were correlated with lake area over a 1°×1° grid using aggregated (mean or summed) values for HMA regions. A statistically

https://doi.org/10.5194/essd-2020-57
Preprint. Discussion started: 15 April 2020

significant positive correlation exists between lake area and debris-covered glacial area of different regions (R^2=0.27, Table A6). Correlations and significance levels strengthen if the Karakoram— where few lakes exist— is excluded. Glacier length and debris cover are strongly correlated (R^2=0.76, Table A5), reflecting abundant debris on most large low-gradient valley glaciers in HMA; in turn, debris-covered, low-gradient glaciers favor supraglacial and proglacial lake formation. Glaciers are generally longest and most heavily debris covered in the Hindu Kush-Himalaya (Fig. 6a and Fig. 6b). A direct correlation between lake area and glacier length is, however, weak (R^2=0.14, Table A6).

Some adjacent regions have comparable amounts of large debris-covered glaciers but substantial differences in total lake area and area-growth rates (Gardelle et al., 2011). Regional differences in longer-term climate trends could play a role, with Nyainqentanglha, Central and Eastern Himalayan regions all characterized by rapid warming and decreased precipitation since 1979 (Fig. 6c and Fig. 6d), favoring negative glacial mass balances (Nie et al., 2017). This plausibly explains why lake area is typically larger in these regions relative to adjacent regions further west and north despite often similar glacier characteristics (in terms of debris cover and glacier length) (Fig. 6e and Fig. 6f). Further, there is very little debris covered area but rapid warming in Eastern Himalaya (Fig. 6f). The Karakoram is an anomaly of positive glacier mass balances and glacier advances (Gardelle et al., 2012) and also anomalously small area of proglacial lakes (Fig. 6f). These results suggest that regional geographic variability of debris cover, that is likely influenced by geological conditions, together with trends in warming and precipitation over the past few decades, influenced the overall distribution of proglacial and supraglacial lake area in their current states across HMA (Haritashya et al., 2018;Scherler et al., 2018;Dan and CLAGUE, 2011;Bo et al., 2019).

https://doi.org/10.5194/essd-2020-57
Preprint. Discussion started: 15 April 2020

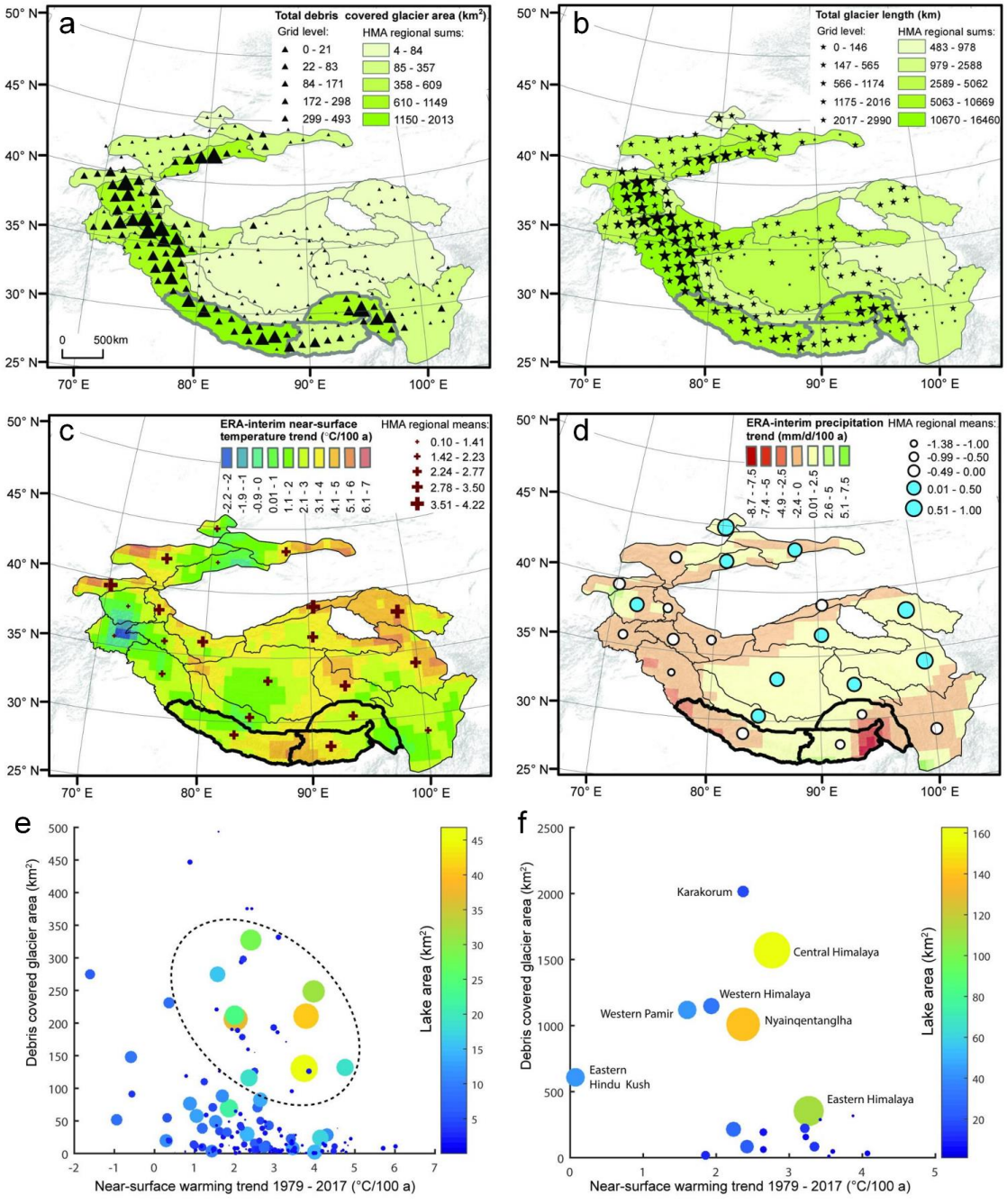

Fig. 6. Geomorphic and climatic influences on lake distribution. (a) Debris-covered area and **(b)** glacier length aggregated on a 1°×1° grid. Linear trends in **(c)** temperature and **(d)** precipitation calculated for 1979-2017 from ERA-Interim, including aggregated means over HMA regions. Relationship between total debris-covered area, near-surface temperature warming, and proglacial and supraglacial lake area of 2017 in **(e)** 1°×1° grid tiles and **(f)** HMA regions. Some regions discussed in the

https://doi.org/10.5194/essd-2020-57
Preprint. Discussion started: 15 April 2020


Open Access Earth System Science Data Discussions

text are labelled. The lake coverage is high in areas of both rapid warming and high debris cover (E, dashed ellipse). Dot sizes are proportional to lake area. See supplementary material for details on data sources.

6 Discussions

6.1 Comparison with other lake dataset

Hi-MAG was compared with recent Landsat-based lake inventories (Nie et al., 2017;Zhang et al., 2015;Pekel et al., 2016). Hi-MAG lake number was 4,537 higher and area was 722.42 km^2 higher than previously estimated for the Tibetan Plateau. The largest discrepancy is in the Gangdise, Himalaya and Nyainqentanglha Mountains in 2010 (Zhang et al., 2015). Across the Himalaya, we found 529.54 km^2 of glacial lakes, 16.3% more than previous estimates in 2015 (Nie et al., 2017). Hi-MAG also showed a much larger lake area than in the Global Surface Water (GSW) dataset, which is the only publicly available high-resolution surface water dataset over HMA.

We compared the lake extent between GSW and our Hi-MAG database summed by mountain range in 2015. GSW data are available at https://global-surface-water.appspot.com/download. For the sake of a reliable comparative analysis, glacial lakes in the GSW were further extracted using the range of glacier buffer (10 km) polygons. Hi-MAG represented more glacial lakes in the Himalaya, Eastern Hindu Kush, and Tien Shan, and fewer in Eastern Pamir and Western Kunlun Shan. Fig. A5 illustrates the differences between our Hi-MAG glacial lake results and GSW-derived lake area for the whole HMA region.

The glacial lake area observed in our lake dataset in the Eastern Pamir and Western Kunlun Mountains does not conform to the glacial lake definitions applied in the GSW for these sub-regions. While there is a significant number of glacial lakes from an open water perspective, only part of lakes are formed by glacier meltwater, the main criterion used in our estimates. Additionally, the Himalaya, Eastern Hindu Kush, and some other Tien Shan host thousands of glacial lakes that are not readily observable in the GSW product. Large discrepancies in mountainous glacial lake estimates preclude a significant consistency between GSW and our Hi-MAG lake data over the HMA region. The region with the highest consistency between GSW and Hi-MAG product is interior Tibet. There is little agreement for Tien Shan, which reflects the difficult nature of mapping glacial lakes in environments with similar reflectance from the adjacent land surfaces, so errors could exist in either dataset, but we also did a detailed manual editing, so we were not relying exclusively on automatic classification. Karakoram regions have fewer glacial lakes in our estimate.

The little agreement between our Hi-MAG glacial lakes data and GSW data is mainly due to its lack of systematic glacial lake inventories and mapping capabilities. The lake dynamics and differing climate contexts within HMA may also lead to inconsistencies between the sub-regions. Hi-MAG might have made better use of the optimum satellite imaging season to map glacial lakes, potentially resulting in more complete mapping by avoiding conditions — such as periods of lake ice — that may confound mapping.

6.2 Known issues and planned improvements

There are several important issues and limitations to the datasets produced and methods used within this study that are important to highlight to potential users. (i) Bodies of water smaller than nine connected pixels (e.g., 1 x 9 pixels or 3 x 3 pixels, corresponding to 30 x 270 m or 90 x 90 m, respectively), those obscured by frozen water surface and loose moraines or hidden by terrain shadows were not included. Broken floating ice or isolated moraine that stand in open water for some times were mapped. Supraglacial lakes such as melt ponds developed on the surface of glaciers present particular challenges because of their small size and highly dynamic properties. Most supraglacial lakes are transient or seasonal, or at least fluctuate

https://doi.org/10.5194/essd-2020-57
Preprint. Discussion started: 15 April 2020

seasonally, as they commonly drain and may refill, but in fact this short-duration seasonal water more generally is likely to be underestimated because of temporal discontinuities in the archive and gaps caused by persistent cloud cover. (ii) The spatial and temporal information reported in the Landsat dataset used in this study complements that acquired in the past. Nevertheless, the biggest limitation to glacial lake mapping from these data are undoubtedly the geographic and temporal discontinuities of the Landsat archive itself. Historical data over the entire HMA before 2008 can be recovered partly from the Landsat 4 TM/MSS, Landsat 5 TM, Landsat 7 ETM+, and partly from SPOT, and other satellite systems, etc., although data access is not always at the full, free and open level of Landsat. In this regard, ASTER is freely accessible and has higher resolution than Landsat, but the temporal coverage is very limited in most of HMA. Other Landsat-like moderate resolution multi-spectral sources could be also used to improve and extend the temporal sampling. For example the European Space Agency's Sentinel 2a satellite launched in 2015 and provides optical imagery at 10 m resolution, which will benefit future research combing all available satellite observations with GEE cloud computing power would make long-term monitoring of changes to HMA's glacial lakes and inland waters possible.

7 Data availability

The Hi-MAG database is distributed under a Creative Commons Attribution 4.0 License. The data can be downloaded from the data repository Zenodo at https://doi.org/10.5281/zenodo.3700282 (Chen et al., 2020).

8 Conclusions

In conclusion, the Hi-MAG dataset and others have turned to Earth observation satellite data, especially Landsat imagery, to provide a more consistent delineation of large-scale glacial lake changes. Some remote-sensed glacial lake mapping methods have enabled local-scale area estimation or spatial representation of lake extent and change. Such methods result in relatively good performance for areas having simple lake characteristics and environmental backgrounds, but do not allow for continental-scale glacial lake mapping characterized by diverse climatic conditions, physical properties and surrounding environments. Automated methods for the extraction of glacial lakes over the large-scale areas are further developed in our work. However, visual interpretation and manual editing is still an effective way to ensure the high accuracy of lake inventories and appended attributed information for further analysis.

Mapping of glacial lakes across the Tibetan Plateau and adjoining ranges reveals a complex pattern of lake occurrence and growth/shrinkage. Small proglacial and unconnected lakes contributed more than half of lake area expansion in some regions. Proglacial lake growth is proceeding at high elevations, but glacier retreat and lake disconnections are also starting to occur at higher elevations, causing the number and area of both classes to increase. At low elevations, few glaciers remain where proglacial lakes can form, and already detached lakes lack growth mechanisms. Overall, continued growth of glacial lakes can be expected, particularly where large debris covered tongues remain.

This freely-downloadable, detailed Hi-MAG dataset can also be used in future studies to provide a sound and consistent basis on which to quantify critical relationships and processes in HMA, including glacier-climate-lake interactions, glacio-hydrologic models, glacial lake outburst floods and potential downstream risks and water resources.

https://doi.org/10.5194/essd-2020-57
Preprint. Discussion started: 15 April 2020

Open Access Earth System Science Data Discussions

Appendix A

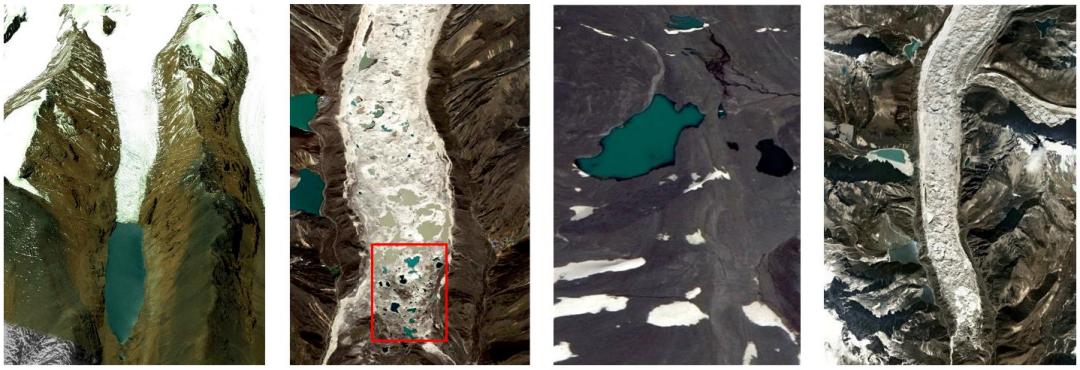

Fig. A1. Examples of the various types of glacial lake found in the HMA: (a) pro-glacial lakes, which are connected to the parent glacier and usually impounded by a debris dam (usually a moraine or ice-cored moraine); (b) supraglacial lakes (denoted by the red rectangle) which develop on the glacier surface; (c) unconnected glacial lakes; and (d) ice-marginal lakes that distributed on the edge of a glacier. Background images were acquired from © Google Earth.

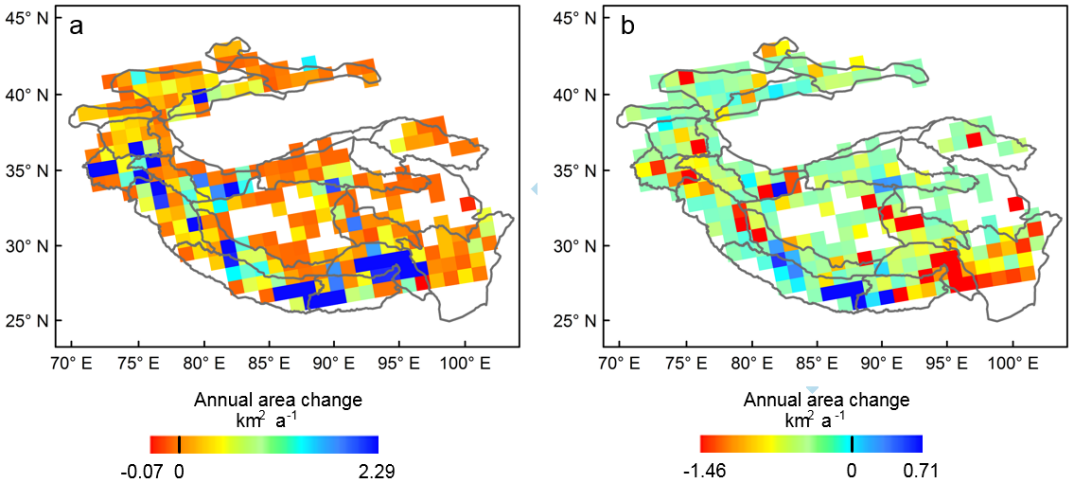

Fig. A2. Annual changes in lake area between 2008 and 2017 on a 1°×1° grid. The (a) upper and (b) lower slopes represent the 90% confidence interval.

https://doi.org/10.5194/essd-2020-57
Preprint. Discussion started: 15 April 2020

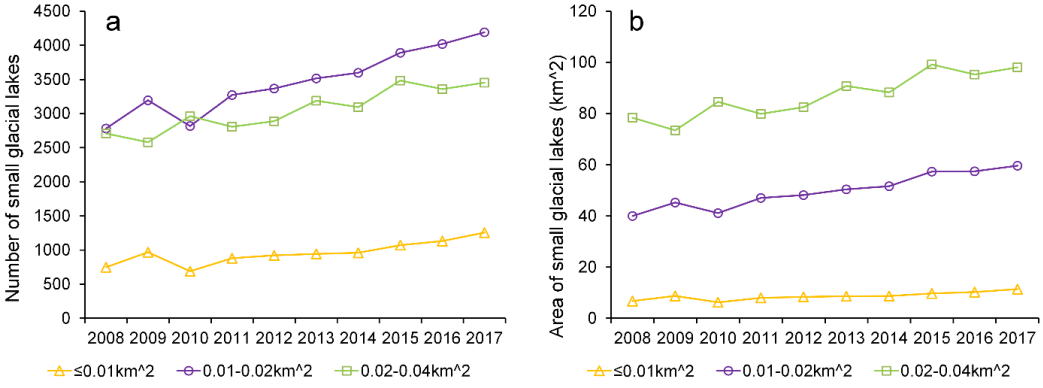

370 **Fig. A3. Changes in the (a) number and (b) area of small glacial lakes in HMA during 2008-2017.**

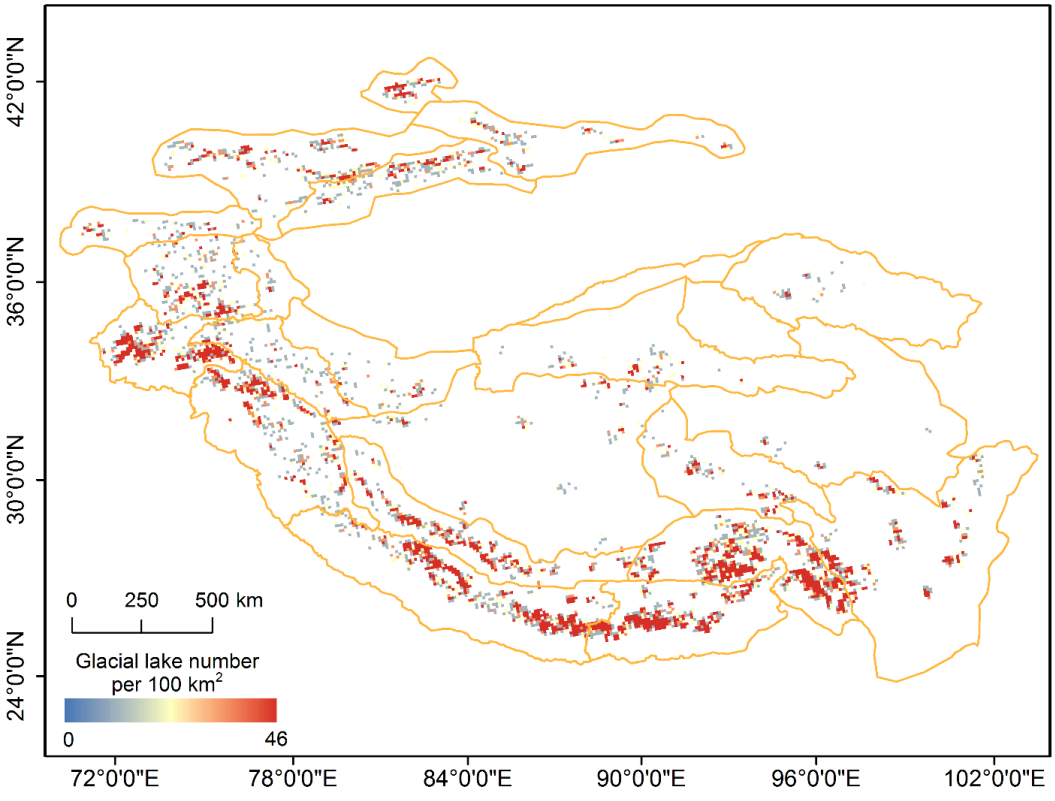

Fig. A4. Density (number per 100 km^2) distribution of glacial lakes in 2017.

https://doi.org/10.5194/essd-2020-57
Preprint. Discussion started: 15 April 2020

Open Access Earth System Science Data Discussions

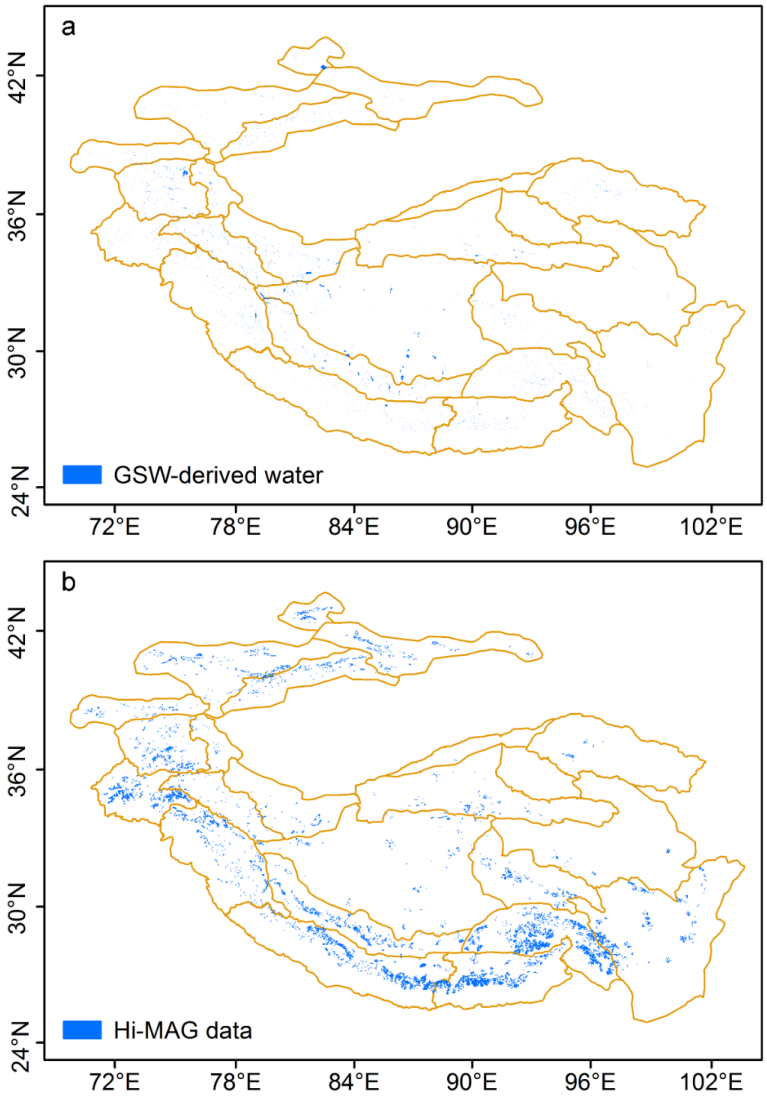

375 **Fig. A5. Comparison of the glacial lake measured in the global maps of (a) Pekel et al.23. and (b) our Hi-MAG data.**

https://doi.org/10.5194/essd-2020-57
Preprint. Discussion started: 15 April 2020

Open Access Earth System Science Data Discussions

Table A1. Mountain-wide glacial lake number and area per year and total loss/gain from 2008 to 2017. The unit of area is km^2.

Mountain range	2008		2009		2010		2011		2012		2013		2014		2015		2016		2017		Total gain/loss (2008-2017)	
	No.	Area	No.	Area	No.	Area	No.	Area	No.	Area	No.	Area	No.	Area	No.	Area	No.	Area	No.	Area	No.	Area
Eastern Hindu Kush	1153	67.85	530	36.02	1045	65.04	929	61.82	919	55.93	1199	67.11	1137	67.66	1148	64.64	1222	64.7	1391	70.71	238	2.86
Western Himalaya	851	100.57	776	87.23	650	87.6	661	84.98	653	82.41	713	88.06	878	109.44	788	101.08	1069	107.36	980	104.03	129	3.46
Eastern Himalaya	1607	195.88	1458	171.58	1552	189.31	1820	206.47	1842	204.39	1794	202.92	1824	202.67	2117	224.4	1904	211.79	1908	213.39	301	17.51
Central Himalaya	1028	166.18	1527	167.13	1380	177.85	1733	189.06	1667	187.6	1600	187.33	1729	192.11	1995	204.06	2026	202.65	2120	205.04	1092	38.86
Karakoram	107	14.15	166	13.73	172	15.64	101	11.53	100	11.15	143	12.95	116	12.27	144	14.86	227	17.39	206	17.82	99	3.67
Western Pamir	413	80.24	435	77.93	487	82.93	512	95.01	443	91.66	492	92.37	523	97.19	521	94.5	531	96.6	592	90.96	179	10.72
Eastern Pamir	22	4.22	35	5.02	38	5.22	33	4.45	45	5.21	34	4.78	40	4.63	42	5.16	52	5.36	48	5.33	26	1.11
Pamir Alay	121	10.72	67	9.33	94	10.75	131	11.67	126	11.39	123	11.54	127	11.5	135	11.61	129	11.35	129	11.97	8	1.25
Northern/Western Tien Shan	451	33.36	296	29.06	466	33.69	526	37.58	500	31.96	493	31.55	545	43.33	500	32.31	485	34.67	606	37.03	155	3.67
Central Tien Shan	279	26.58	204	26.56	286	31.52	320	34.38	320	34.43	312	31.26	316	35.13	311	34.22	425	35.1	462	36.2	183	9.62
Eastern Tien Shan	231	14.5	217	16.67	228	14.98	239	14.94	237	14.45	247	14.85	237	14.48	287	15.65	221	16.43	226	16.28	-5	1.78
Western Kunlun Shan	36	84.15	95	92.64	87	91.64	76	93.78	73	87.5	122	97.55	81	92.49	89	95.34	112	96.01	118	101.49	82	17.34
Eastern Kunlun Shan	88	6.8	99	6.87	168	12.62	183	12.84	199	13.17	188	12.1	200	13.13	261	16.25	217	12.09	208	13.87	120	7.07
Gangdise Mountains	687	129.01	822	131.34	761	128.29	844	126.4	834	126.05	858	128.01	900	130.93	969	131.26	1023	134.26	1076	134.71	389	5.7
Hengduan Shan	1012	70.09	1046	59.55	878	58.96	689	50.82	824	55.41	953	59.22	911	61.16	949	59.13	860	57.38	887	59.12	-125	-10.97
Tibetan Interior Mountains	189	124.72	230	128.95	258	129.39	249	125.24	238	128.78	238	131.18	243	133.52	280	130.58	238	124.99	236	128.05	47	3.33
Eastern Tibetan Mountains	28	13.82	29	10.06	46	13.57	73	18.3	52	11.23	52	11.78	54	13.22	49	11.74	42	8.39	38	8.46	10	-5.36
Tanggula Shan	477	72.66	223	57.82	261	63.75	230	59.51	267	59.88	277	60.9	267	59.99	430	68.15	273	62.31	269	62.25	-208	-10.41
Qilian Shan	65	6.95	53	5.02	58	5.59	46	5.02	52	5.23	49	4.78	64	5.53	49	4.78	60	5.5	57	5.15	-8	-1.8
Dzhungarsky Alatau	278	13.18	207	11.17	222	11.46	265	12.35	251	12.2	263	12.51	261	11.63	191	11.18	225	10.33	255	12.35	-23	-0.83

https://doi.org/10.5194/essd-2020-57
Preprint. Discussion started: 15 April 2020

Open Access Earth System Science Data Discussions

Nyainqentanglha	2401	302.03	2620	271.56	2453	282.7	2433	287.43	2552	285.32	2685	285.98	2562	292.46	2888	294.9	2542	289.72	2665	301.67	264	-0.36

https://doi.org/10.5194/essd-2020-57
Preprint. Discussion started: 15 April 2020

Open Access Earth System Science Data Discussions

Table A2. Mountain-wide area loss/gain between 2008 and 2017, and area change rate from 2008 to 2017 for various lake types and sizes. Supraglacial and ice-marginal lakes have relative few coverage areas and are not listed details in the table. Total area gain/loss (2008-2017) includes area information on supraglacial and ice-marginal lakes. The unit of area and change rate is km2 and km2a-1, respectively. '-' indicates invalid data for specific years.

Mountain range	Total area gain/loss (2008-2017)	Small proglacial lakes		Small unconnected lakes		Medium/large proglacial lakes		Medium/large unconnected lakes	
		Area gain/loss (2008-2017)	Area change rate	Area gain/loss (2008-2017)	Area change rate	Area gain/loss (2008-2017)	Area change rate	Area gain/loss (2008-2017)	Area change rate
Eastern Hindu Kush	2.86	1.44	0.3	1.97	0.39	-0.43	0.53	-0.04	0.3
Western Himalaya	3.46	1.24	0.19	1.35	0.19	0.83	0.62	0.24	0.91
Eastern Himalaya	17.51	2.8	0.32	2.4	0.38	23.46	2.62	-9.75	0.34
Central Himalaya	38.86	8.43	0.78	6.89	0.52	17.15	2.31	6.07	0.7
Karakoram	3.67	0.7	0.06	0.44	0.03	2.63	0.2	0.18	0.09
Western Pamir	10.72	1.94	0.15	0.49	0.04	2.43	0.28	5.7	1.28
Eastern Pamir	1.11	0.19	0.0125	0.08	0.002	0.7	0.03	-0.006	-0.004
Pamir Alay	1.25	-0.16	0.04	0.09	0.01	-0.02	0.011	1.32	0.11
Northern/Western Tien Shan	3.67	1.58	0.19	0.59	0.06	1.2	0.2	0.27	0.04
Central Tien Shan	9.62	1.56	0.16	0.57	0.07	3.61	0.31	3.39	0.36
Eastern Tien Shan	1.78	0.15	0.03	-0.08	-0.003	-0.6	-0.05	2.21	0.1
Western Kunlun Shan	17.34	0.11	-0.0007	0.41	0.04	1.4	0.04	15.42	1.15
Eastern Kunlun Shan	7.07	0.43	0.04	0.7	0.11	2.7	0.313	3.21	0.24
Gangdise Mountains	5.7	3.98	0.39	1.66	0.15	-1.63	0.0041	2.02	0.08
Hengduan Shan	-10.97	-0.51	0.02	-0.41	-0.1	-6.36	-0.28	-1.72	0.003
Tibetan Interior Mountains	3.33	0.41	0.02	0.43	0.03	0.21	-0.0001	2.57	0.17
Eastern Tibetan Mountains	-5.36	-	-	-0.097	-0.008	-0.07	-0.01	-5.61	-0.53
Tanggula Shan	-10.41	-0.26	0.02	-2.68	-0.07	0.44	0.07	-7.69	-0.24
Qilian Shan	-1.8	0.07	0.0013	-0.17	-0.0007	2.26	0.11	-3.95	-0.2
Dzhungarsky Alatau	-0.83	-0.31	-0.01	-0.09	-0.02	-0.6	-0.03	0.13	-0.05
Nyainqentanglha	-0.36	3.75	0.42	2.44	0.07	4.62	1.36	-7.26	-0.45
The whole HMA region	98.22	27.54	3.23	16.98	1.93	53.93	8.66	6.7	6.81

https://doi.org/10.5194/essd-2020-57
Preprint. Discussion started: 15 April 2020

Open Access Earth System Science Data Discussions

385 **Table A3. Mountain-wide annual glacial lake area from 2008 to 2017 for small proglacial lakes, medium/large proglacial lakes, small unconnected lakes and medium/large unconnected lakes. The unit of area is km2. '-' indicates invalid data for specific years. Acronyms are used to represent the name of mountain ranges to save space.**

		EHK	WH	EH	CH	K	WP	EP	PA	N/WT	CT	ET	WK	EK	G	H	TIM	ETM	T	Q	DA	N	Total
Small proglacial lakes	2008	7.07	6.64	6.52	6.02	0.66	3.17	0.05	1.35	4.15	2.43	2.50	0.04	0.14	4.18	4.27	0.35	-	1.56	0.25	2.83	8.76	63.94
	2009	2.67	6.54	7.17	9.78	1.12	3.65	0.30	0.49	2.67	1.94	2.55	0.23	0.34	5.85	3.75	0.73	0.08	0.90	0.44	2.10	9.73	63.03
	2010	6.50	4.97	7.73	8.80	1.00	4.21	0.31	0.68	4.42	2.78	2.86	0.27	0.61	5.81	3.46	0.96	0.15	1.28	0.54	2.16	9.90	69.40
	2011	5.51	4.62	8.25	12.17	0.74	4.60	0.23	1.29	4.88	2.81	2.72	0.09	0.34	6.40	2.67	0.99	0.40	1.02	0.28	2.50	9.94	72.45
	2012	5.04	4.77	8.78	11.23	0.62	4.00	0.32	1.31	5.18	3.13	2.88	0.11	0.34	7.01	3.34	0.83	0.41	1.42	0.41	2.62	11.59	75.34
	2013	7.38	5.74	8.87	10.24	0.97	4.47	0.16	1.21	4.98	3.08	3.12	0.26	0.36	6.59	4.57	0.65	0.34	1.43	0.41	2.76	11.86	79.45
	2014	6.47	6.62	8.75	11.87	0.78	4.40	0.30	1.30	5.02	2.89	2.86	0.08	0.35	7.07	3.62	0.85	0.41	1.38	0.57	2.84	11.57	80.00
	2015	6.43	5.89	9.93	13.68	1.25	4.57	0.30	1.37	4.95	3.03	3.53	0.15	0.72	7.71	4.53	1.08	0.30	1.75	0.41	1.80	13.00	86.38
	2016	7.33	7.88	9.33	14.19	1.43	4.65	0.35	1.19	4.71	3.55	2.64	0.15	0.68	8.45	3.57	0.79	0.45	1.36	0.35	2.35	11.96	87.36
	2017	8.51	7.88	9.32	14.45	1.36	5.11	0.24	1.19	5.73	3.99	2.64	0.15	0.58	8.16	3.76	0.76	0.42	1.30	0.32	2.52	12.51	90.90
Small unconnected lakes	2008	7.81	2.45	8.79	2.38	0.14	0.96	0.01	0.17	1.52	1.24	0.41	0.10	1.14	3.91	7.87	1.37	0.14	4.23	0.39	0.63	11.62	57.28
	2009	3.70	2.88	8.32	6.68	0.22	0.90	0.07	0.09	0.98	0.71	0.38	0.32	0.87	4.27	9.91	1.50	0.08	1.45	0.03	0.62	18.11	62.09
	2010	6.97	2.34	8.18	5.28	0.32	1.16	0.10	0.27	1.68	1.02	0.34	0.22	1.34	4.00	7.90	1.73	0.18	1.29	-	0.66	15.07	60.05
	2011	6.03	1.89	10.70	6.36	0.13	1.03	0.02	0.16	1.88	1.23	0.47	0.22	1.79	4.23	5.72	1.92	0.21	1.51	0.02	0.66	13.58	59.76
	2012	6.01	1.97	11.05	6.33	0.11	0.72	0.02	0.13	1.66	0.92	0.31	0.19	1.91	3.97	6.98	1.67	0.10	1.66	0.03	0.65	14.22	60.61
	2013	8.08	2.34	10.36	6.78	0.16	1.16	0.05	0.23	1.80	0.92	0.27	0.67	1.68	4.54	7.72	1.66	0.09	1.65	0.01	0.70	16.70	67.57
	2014	7.67	2.72	10.71	6.52	0.11	1.23	0.04	0.15	2.07	1.06	0.31	0.25	1.92	4.45	7.70	1.67	0.16	1.63	0.07	0.70	14.19	65.33
	2015	7.80	3.07	12.45	8.02	0.30	1.10	0.02	0.20	1.88	0.93	0.46	0.28	2.34	4.83	7.66	2.07	0.09	3.55	0.01	0.58	18.41	76.05
	2016	8.81	4.80	11.27	8.11	0.37	1.16	0.07	0.29	1.52	1.74	0.40	0.60	1.98	5.08	7.26	1.63	0.09	1.56	0.22	0.30	13.76	71.02
	2017	9.78	3.80	11.19	9.27	0.58	1.45	0.09	0.26	2.11	1.81	0.33	0.51	1.84	5.57	7.46	1.80	0.05	1.55	0.22	0.54	14.06	74.27
Medium/ large proglacial lakes	2008	34.82	27.90	84.21	118.75	6.76	29.23	3.94	2.68	12.90	10.69	5.41	3.90	0.38	17.22	16.81	1.82	1.38	8.83	1.73	7.94	142.33	539.63
	2009	20.52	18.75	83.68	112.12	7.86	28.79	4.64	2.05	10.15	11.11	5.13	5.26	0.54	13.03	8.60	3.10	0.96	8.44	4.17	6.72	114.66	470.28
	2010	33.04	20.18	96.68	125.71	8.26	31.18	4.50	2.70	12.15	13.64	6.05	5.16	1.64	16.09	9.75	2.76	1.18	10.17	4.48	6.89	125.63	537.84
	2011	34.34	25.04	104.85	127.99	6.96	30.19	3.96	2.63	14.20	12.39	5.68	4.11	3.03	14.63	8.14	2.36	2.69	9.29	3.95	7.52	135.03	558.98
	2012	30.05	22.95	102.55	129.33	6.73	29.99	4.55	2.42	12.79	13.5	5.67	3.43	3.13	14.36	8.40	2.72	1.31	8.88	4.06	7.23	131.11	545.16
	2013	33.72	22.47	104.01	129.48	7.07	29.63	4.19	2.71	11.58	13.42	6.13	4.79	2.65	13.95	9.25	2.51	1.31	9.40	4.12	7.17	125.06	544.62
	2014	35.48	29.43	100.11	130.3	6.95	30.61	4.03	2.67	15.17	14.16	5.72	4.49	3.13	14.94	9.54	2.72	1.31	9.46	4.16	7.26	134.48	566.12
	2015	33.12	25.48	111.49	136.87	8.63	32.73	4.55	2.50	12.29	12.98	5.94	4.42	3.73	15.61	9.25	3.17	1.31	10.33	4.12	7.16	127.37	573.05
	2016	32.57	26.76	106.6	135.76	8.95	31.14	4.57	2.44	12.98	13.53	4.65	4.65	2.98	15.49	9.61	2.41	1.31	9.27	3.99	6.70	140.67	577.03
	2017	34.39	28.73	107.67	135.9	9.39	31.66	4.64	2.66	14.10	14.30	4.81	5.30	3.08	15.59	10.45	2.03	1.31	9.27	3.99	7.34	146.95	593.56

https://doi.org/10.5194/essd-2020-57
Preprint. Discussion started: 15 April 2020

Open Access Earth System Science Data Discussions

Medium/ large unconnected lakes	2008	17.95	62.39	93.94	34.00	5.48	46.73	0.21	6.51	14.76	12.08	6.14	80.07	5.13	103.35	39.15	120.88	12.28	57.76	4.56	1.71	134.53	859.61
	2009	9.07	58.27	71.86	34.89	3.58	44.20	-	6.69	15.23	12.78	8.54	86.75	5.06	108.18	37.25	123.60	8.93	47.01	0.37	1.72	128.34	812.32
	2010	18.37	59.27	76.14	34.54	4.25	46.03	0.29	7.08	15.42	13.99	5.68	85.97	8.98	102.36	37.82	123.91	12.05	51.00	0.56	1.73	131.33	836.77
	2011	15.78	52.54	82.02	38.10	3.31	58.91	0.17	7.58	16.58	17.88	6.03	89.34	7.65	101.12	34.27	119.95	14.98	47.66	0.75	1.56	128.28	844.46
	2012	14.73	51.86	81.08	35.98	3.07	56.76	0.17	7.51	12.29	16.69	5.46	83.76	7.74	100.69	36.66	123.53	9.39	47.86	0.71	1.60	127.52	825.06
	2013	17.78	56.69	78.9	36.43	3.40	56.86	0.28	7.36	13.14	13.72	5.20	91.76	7.34	102.91	37.67	126.28	10.03	48.38	0.23	1.77	131.58	847.71
	2014	17.87	69.71	82.2	39.02	3.77	60.64	0.17	7.36	21.01	16.83	5.46	87.66	7.68	104.46	40.29	128.20	11.32	47.47	0.71	0.72	131.27	883.82
	2015	17.18	65.76	89.15	40.11	4.35	55.82	0.17	7.51	13.16	17.16	5.58	90.47	9.40	103.09	37.67	124.23	10.03	52.47	0.23	1.61	135.18	880.33
	2016	15.85	66.88	83.55	39.18	5.32	59.39	0.20	7.40	15.42	15.68	8.62	90.53	6.42	105.23	36.92	120.15	6.53	50.07	0.92	0.86	122.44	857.56
	2017	17.91	62.63	84.19	40.07	5.66	52.43	0.20	7.83	15.03	15.47	8.35	95.49	8.34	105.37	37.43	123.45	6.67	50.07	0.61	1.84	127.27	866.31

https://doi.org/10.5194/essd-2020-57
Preprint. Discussion started: 15 April 2020

Open Access Earth System Science Data Discussions

390 **Table A4. Statistics of area of small glacial lakes in each mountain range for the year of 2017.**

Mountain range	≤0.01km^2	0.01-0.02km^2	0.02-0.04km^2	Total (≤0.04km^2)	Total (% of the total lake area for all size classes)
Eastern Hindu Kush	0.99	6.52	10.86	18.37	25.98
Western Himalaya	0.81	4.35	6.94	12.1	11.63
Eastern Himalaya	0.97	7.57	12.34	20.88	9.78
Central Himalaya	1.98	9.33	13.57	24.88	12.13
Karakoram	0.12	0.98	1.3	2.4	13.47
Western Pamir	0.69	2.43	3.62	6.74	7.41
Eastern Pamir	0.05	0.18	0.2	0.43	8.07
Pamir Alay	0.11	0.46	0.88	1.45	12.11
Northern/Western Tien Shan	0.71	2.98	4.19	7.88	21.28
Central Tien Shan	0.76	2.3	3.36	6.42	17.73
Eastern Tien Shan	0.28	1.02	1.71	3.01	18.49
Western Kunlun Shan	0.03	0.28	0.38	0.69	0.68
Eastern Kunlun Shan	0.16	1.05	1.22	2.43	17.52
Gangdise Mountains	1.04	5.19	7.5	13.73	10.19
Hengduan Shan	0.68	3.86	6.69	11.23	19.00
Tibetan Interior Mountains	0.17	0.87	1.52	2.56	2.00
Eastern Tibetan Mountains	0.02	0.18	0.27	0.47	5.56
Tanggula Shan	0.27	1	1.63	2.9	4.66
Qilian Shan	0.04	0.17	0.32	0.53	10.29
Dzhungarsky Alatau	0.23	1.05	1.84	3.12	25.26
Nyainqentanglha	1.21	7.83	17.7	26.74	8.86

https://doi.org/10.5194/essd-2020-57
Preprint. Discussion started: 15 April 2020

Open Access Earth System Science Data Discussions

Table A5. Summary of correlation coefficients (*R*) for key lake, topographic, geomorphic and climatological parameters, calculated within 1°×1° grid cells across HMA. Correlation coefficients are bold where $p < 0.05$; (*) indicates $p < 0.01$.

	Lake area (2008)	Lake area (2017)	Lake change (2008 – 2017)	Glacier (gl.) area	Debris-covered gl. area	Total gl. length	Mean gl. slope	Mean gl. elevation	Temperature change 1979 – 2017	Precipitation change 1979 – 2017
Lake area (2008)	1.00									
Lake area (2017)	**0.97***	1.00								
Lake change (2008 – 2017)	**0.73***	**0.80***	1.00							
Glacier (gl.) area	**0.17**	**0.18**	**0.20**	1.00						
Debris-covered gl. area	**0.30***	**0.30***	**0.28***	**0.86***	1.00					
Total gl. length	**0.26***	**0.27***	**0.27***	**0.90***	**0.87***	1.00				
Mean gl. Slope	0.07	0.04	-0.02	-0.02	0.14	-0.01	1.00			
Mean gl. Elevation	**0.19**	**0.21**	**0.24***	0.15	0.07	0.12	-0.11	1.00		
Temperature change 1979 – 2017	-0.03	-0.01	0.01	-0.15	**-0.22***	**-0.26***	0.05	0.02	1.00	
Precipitation change	-0.06	0.01	0.14	-0.08	-0.13	-0.10	**-0.18**	0.15	0.15	1.00

395

https://doi.org/10.5194/essd-2020-57
Preprint. Discussion started: 15 April 2020

Open Access Earth System Science Data Discussions

Table A6. Regional summary of key topographic, geomorphic and climatological parameters compared to pro- and supraglacial lake area in 2017. Correlation coefficients are bold where $p < 0.05$; (*) indicates $p < 0.01$.

Region	Total area (km^2)	Lake area (km^2)	Glacier (gl.) area (km^2)	Debris-covered gl. area (km^2)	Total gl. length (km)	Mean gl. slope (°)	Mean gl. elevation (m)	Temperature change 1979 – 2017 (°C/century)	Precipitation change 1979 – 2017
Central Himalaya	189494	33.0	7986	1149	10669	24	5542	2.77	-0.25
Dzhungarsky Alatau	37542	9.9	521	18	978	24	3615	1.85	0.74
Eastern Himalaya	254886	162.7	8678	1567	3614	26	5484	3.26	-0.84
Eastern Hindu Kush	39605	1.4	2118	291	5062	27	4856	0.08	-0.86
Eastern Kunlun Shan	123388	5.5	8457	159	3384	26	5389	3.60	0.06
Eastern Pamir	109239	41.9	8417	1118	2364	27	5064	3.42	-0.50
Eastern Tibetan Mountains	372649	28.1	1281	212	483	23	5345	3.55	0.73
Eastern Tien Shan	140900	7.6	2332	193	3977	28	3974	2.65	0.17
Gangdise Mountains	526111	5.9	3815	59	2570	23	5892	2.42	0.33
Hengduan Shan	145064	12.1	1841	84	2048	21	5278	2.24	-0.13
Karakoram	201699	4.3	1598	30	16460	26	5399	2.37	-0.35
Northern/Western Tien Shan	105456	25.7	7270	842	4138	27	3943	3.22	-0.36
Nyainqentanglha	154884	22.8	1271	80	8710	24	5282	2.37	-1.00

https://doi.org/10.5194/essd-2020-57
Preprint. Discussion started: 15 April 2020

Pamir Alay	187275	11.5	2262	223	3441	23	4109	3.88	-0.27
Qilian Shan	333123	1.6	312	12	2588	24	4847	4.07	0.51
Tanggula Shan	172746	138.8	7047	1011	1893	25	5521	3.34	0.46
Tibetan Interior Mountains	256729	2.9	2995	45	4179	24	5927	2.64	0.31
Western Himalaya	95404	42.8	2938	609	11974	25	5180	1.93	-1.24
Western Kunlun Shan	164785	111.3	2838	357	8108	24	5642	3.22	-0.55
Western Pamir	71845	1.1	1847	319	11640	25	4844	1.61	0.08
Lake area: Correlation Coefficient (*R*)			0.23	**0.52**	0.37	0.02	0.26	-0.19	**-0.46**
Exl. Karakoram			**0.52**	**0.75***	**0.53**	0.11	0.27	-0.22	**-0.47**

https://doi.org/10.5194/essd-2020-57
Preprint. Discussion started: 15 April 2020

Author contributions. FC: conceptualization, methodology, lake evolution analysis, project administration, resources, and writing; MMZ: conceptualization, methodology, lake evolution analysis, validation, and writing; HDG: funding acquisition, supervision, and writing; SA: methodology, climate and debris cover analysis, validation, and writing; JSK: analysis, interpretation, and writing; UH: writing and interpretation; CSW: writing.

Competing interests. The authors declare that they have no conflict of interest.

Acknowledgements. We thank T Bolch, and D Shugar for their contributions to this project in its stages of development; L Wang, SG Xu, ZY Lin, H Zhao, YHZ He, TC Shan, ZW Xu, N Wang, ZZ Yin, and JX Wang for cross-validation of data that were so integral to this project. JSK, UKH, and SW contributed gratis, on their own time.

Financial support. This work was supported by the Strategic Priority Research Program of the Chinese Academy of Sciences (XDA19030101), the International Partnership Program of the Chinese Academy of Sciences (131C11KYSB20160061/131211KYSB20170046), and the National Key R&D Program of China (2017YFE0100800).

References

Aparna, S., K., G. P., and Smriti, S.: Evolution of Glacial and High-Altitude Lakes in the Sikkim, Eastern Himalaya Over the Past Four Decades (1975–2017), Frontiers in Environmental Science, 6, 81, 2018.

Bhambri, R., Bolch, T., Kawishwar, P., Dobhal, D. P., Srivastava, D., and Pratap, B.: Heterogeneity in glacier response in the upper Shyok valley, northeast Karakoram, Cryosphere, 7, 1385-1398, 2013.

Bhardwaj, A., Singh, M. K., Joshi, P. K., Snehmani, Singh, S., Sam, L., R.D.Gupta, and RajeshKumar: A lake detection algorithm (LDA) using Landsat 8 data: A comparative approach in glacial environment, International Journal of Applied Earth Observations & Geoinformation, 38, 150-163, 2015.

Bo, Zhao, Yunsheng, Wang, Yonghong, Luo, Ruifeng, Liang, Jia, and Li: Large landslides at the northeastern margin of the Bayan Har Block, Tibetan Plateau, China, Royal Society Open Science, 6, 180844, 2019.

Bolch, T., Kulkarni, A., Kaab, A., Huggel, C., Paul, F., Cogley, J. G., Frey, H., Kargel, J. S., Fujita, K., and Scheel, M.: The State and Fate of Himalayan Glaciers, Science, 336, 310-314, 2012.

Brun, F., Berthier, E., Wagnon, P., Kaab, A., and Treichler, D.: A spatially resolved estimate of High Mountain Asia glacier mass balances from 2000 to 2016, Nature Geoscience, 10, 668-673, 2017.

Chen, J., Zhu, X., E.Vogelmann, J., Gao, F., and Jin, S.: A simple and effective method for filling gaps in Landsat ETM+ SLC-off images, Remote Sensing of Environment, 115, 1053-1064, 2011.

Dan, H. S., and CLAGUE, J. J.: The sedimentology and geomorphology of rock avalanche deposits on glaciers, Sedimentology, 58, 1762-1783, 2011.

Feyisa, G. L., Meilby, H., Fensholt, R., and Proud, S. R.: Automated Water Extraction Index: A New Technique for Surface Water Mapping Using Landsat Imagery, Remote Sensing of Environment, 140, 23–35, 2014.

Gardelle, J., Arnaud, Y., and Berthier, E.: Contrasted evolution of glacial lakes along the Hindu Kush Himalaya mountain range between 1990 and 2009, Global & Planetary Change, 75, 0-55, 2011.

Gardelle, J., Berthier, E., and Arnaud, Y.: Slight mass gain of Karakoram glaciers in the early twenty-first century, Nature Geoscience, 5, 322-325, 10.1038/ngeo1450, 2012.

Gardelle, J., Berthier, E., Arnaud, Y., and Kääb, A.: Region-wide glacier mass balances over the Pamir-Karakoram-Himalaya during 1999–2011, The Cryosphere, 7, 1263-1286, 10.5194/tc-7-1263-2013, 2013.

https://doi.org/10.5194/essd-2020-57
Preprint. Discussion started: 15 April 2020

Hanqiu, X.: Modification of normalised difference water index (NDWI) to enhance open water features in remotely sensed imagery, International Journal of Remote Sensing, 27, 3025-3033, 2006.

Haritashya, U. K., Kargel, J. S., Shugar, D. H., Leonard, G. J., Strattman, K., Watson, C. S., Shean, D., Harrison, S., Mandli, K. T., and Regmi, D.: Evolution and Controls of Large Glacial Lakes in the Nepal Himalaya, Remote Sensing, 10, 798, 2018.

Huan, X., Xin, L., Xiong, X., Haiyan, P., and Xiaohua, T.: Evaluation of Landsat 8 OLI imagery for unsupervised inland water extraction, International Journal of Remote Sensing, 37, 1826-1844, 2016.

Krumwiede, B. S., Kamp, U., Leonard, G. J., Kargel, J. S., and Walther, M.: Recent Glacier Changes in the Mongolian Altai Mountains: Case Studies from Munkh Khairkhan and Tavan Bogd, Global Land Ice Measurements from Space 2014, Springer, Berlin Heidelberg, 2014.

Kumar, S. P.: Estimates of the Regression Coefficient Based on Kendall"s Tau, Publications of the American Statistical Association, 63, 1379-1389, 1968.

Li, J., and Sheng, Y.: An automated scheme for glacial lake dynamics mapping using Landsat imagery and digital elevation models: a case study in the Himalayas, International Journal of Remote Sensing, 33, 5194-5213, 2012.

Liu, J. J., Cheng, Z.-L., and Su, P.-C.: The relationship between air temperature fluctuation and Glacial Lake Outburst Floods in Tibet, China, Quaternary International, 321, 78-87, 2014.

Mueller, N., Lewis, A., Roberts, D., Ring, S., Melrose, R., Sixsmith, J., Lymburner, L., McIntyre, A., Tan, P., Curnowa, S., and Ip, A.: Water observations from space: Mapping surface water from 25years of Landsat imagery across Australia, Remote Sensing of Environment, 174, 341-352, 2016.

Nie, Y., Sheng, Y., Liu, Q., Liu, L., Liu, S., Zhang, Y., and Song, C.: A regional-scale assessment of Himalayan glacial lake changes using satellite observations from 1990 to 2015, Remote Sensing of Environment, 189, 1-13, 2017.

Pekel, J.-F., Cottam, A., Gorelick, N., and Belward, A. S.: High-resolution mapping of global surface water and its long-term changes, Nature, 540, 418-422, 10.1038/nature20584, 2016.

Qiao, L., Wanqin, G., Yong, N., Shiyin, L., and Junli, X.: Recent glacier and glacial lake changes and their interactions in the Bugyai Kangri, Southeast Tibet, Annals of Glaciology, 57, 61-69, 2016.

Quincey, D. J., Richardson, S. D., Luckman, A., Lucas, R. M., Reynolds, J. M., Hambrey, M. J., and Glasser, N. F.: Early recognition of glacial lake hazards in the Himalaya using remote sensing datasets, Global & Planetary Change, 56, 137-152, 2017.

Salerno, F., Thakuri, S., D'Agata, C., Smiraglia, C., Manfredi, E. C., Viviano, G., and Tartari, G.: Glacial lake distribution in the Mount Everest region: Uncertainty of measurement and conditions of formation, Global & Planetary Change, 92-93, 30-39, 2012.

Scherler, D., Wulf, H., and Gorelick, N.: Global Assessment of Supraglacial Debris Cover Extents, Geophysical Research Letters, 45, 11798-11805, 2018.

Song, C., Sheng, Y., Ke, L., Nie, Y., and Wang, J.: Glacial lake evolution in the southeastern Tibetan Plateau and the cause of rapid expansion of proglacial lakes linked to glacial-hydrogeomorphic processes, Journal of Hydrology, 540, 504-514, 2016.

Song, X. P., C, H. M., V, S. S., V, P. P., Alexandra, T., F, V. E., and R, T. J.: Global land change from 1982 to 2016, Nature, 560, 639-643, 2018.

Thakuri, S., Salerno, F., Bolch, T., Guyennon, N., and Tartari, G.: Factors controlling the accelerated expansion of Imja Lake, Mount Everest region, Nepal, Annals of Glaciology, 57, 245-257, 2016.

Thompson, S. S., Benn, D. I., Dennis, K., and Luckman, A.: A rapidly growing moraine-dammed glacial lake on Ngozumpa Glacier, Nepal, Geomorphology 145-146, 1-11, 2012.

Wang, X., Ding, Y. J., Liu, S. Y., Jiang, L. H., Wu, K. P., Jiang, Z. L., and Guo, W. Q.: Changes of glacial lakes and implications in Tian Shan, central Asia, based on remote sensing data from 1990 to 2010, Environmental Research Letters, 8, 575-591, 2013.

Zhang, G., Yao, T., Xie, H., Wang, W., and Yang, W.: An inventory of glacial lakes in the Third Pole region and their changes in response to global warming, Global & Planetary Change, 131, 148-157, 2015.

Zhang, G., Li, J., Zheng, G., and Zhang, G.: Lake-area mapping in the Tibetan Plateau: an evaluation of data and methods, International Journal of Remote Sensing, 38, 742-772, 2017.

https://doi.org/10.5194/essd-2020-57
Preprint. Discussion started: 15 April 2020

485 Zhu, Z., and Woodcock, C. E.: Object-based cloud and cloud shadow detection in Landsat imagery, Remote Sensing of Environment, 118, 83-94, 2012.

Chen, F., Zhang, M., Guo, H., Allen, S., Kargel, J., Haritashya, U., Watson, S.: Annual 30-meter Dataset for Glacial Lakes in High Mountain Asia from 2008 to 2017 (Hi-MAG) [Dataset], Zenodo, https://doi.org/10.5281/zenodo.3700282, 2020.